JOURNAL OF QUATERNARY SCIENCE (2023) 1–14 ISSN 0267-8179. DOI: 10.1002/jqs.3539

JQS Journal of Quaternary Science QRA Quaternary Research Association

On the varied impact of the Storegga tsunami in northwest Scotland

SARAH A. WOODROFFE,[1]* JON HILL,[2] EMMANUEL BUSTAMANTE-FERNANDEZ,[1,3] JERRY M. LLOYD,[1] JAKE LUFF,[1] SARAH RICHARDS[1] and IAN SHENNAN[1]

[1]Department of Geography, Durham University, Durham, UK
[2]Department of Environment and Geography, University of York, York, UK
[3]Department of Earth and Climate Sciences, Tufts University, Medford, MA, USA

Received 13 September 2022; Revised 11 May 2023; Accepted 13 May 2023

ABSTRACT: In this paper we evaluate new data and those from previous studies in northwest Scotland and perform a modelling study to test the hypothesis that the Storegga tsunami (submarine slope failure off the continental shelf of Central Norway dated to 8120–8175 BP) impacted this region. The model used is a 2D non-linear, non-conservative, Shallow Water Equation solver incorporating inundation and realistic glacial isostatic adjustment-corrected palaeobathymetry, with horizontal resolution down to 30 m at sites of interest. The 15 coastal study sites analysed range from south of the Isle of Skye to Assynt. We predict run-up between 2.7 and 9.4 m above contemporaneous mean tide level across the region, with the highest on the west coast of the Outer Hebrides, the east coast of Skye and at the head of long sea lochs east of Skye. We re-evaluate evidence from previously studied open coastal marshes, isolation basins and barrier locations for the tsunami and suggest that in many locations the Storegga tsunami is the most likely cause of erosion, deposition and changes in microfossil assemblages in the early Holocene. The predictions of wave height and inundation produced by the tsunami modelling fit well with the range of available field evidence in the region. We predict significant wave heights at least as far south as Mull on the west coast.

KEYWORDS: coastal basins; microfossils; NW Scotland; Storegga; tsunami

Introduction and aims

The Storegga slide was a massive submarine slope failure off the continental shelf of Central Norway dated 8120–8175 BP (Bondevik et al., 2012, 1997). The slide caused a tsunami that impacted the coastlines of west Norway, Greenland, Faroe Islands and the UK (Bondevik et al., 2005). Although evidence of the tsunami has previously been found on the north and east coasts of Scotland (Dawson et al., 1988; Long et al., 2016; Smith et al., 1985, 2004, 2007), there has been no thorough investigation into evidence for the Storegga tsunami in the northwest region of Scotland. Recent research based on field evidence and tsunami wave modelling indicates that the Storegga tsunami impacted the western part of the north coast of Scotland, at Loch Eribol (Fig. 1) (Long et al., 2016). Their model also predicts that the tsunami propagated further south and west, potentially impacting the Outer Hebrides, the Isle of Skye and the western coastline of the Scottish mainland. Numerous studies of coastal sediments in these areas provide evidence of relative sea-level (RSL) changes since the Last Glacial Maximum, recently summarized along with similar evidence across the rest of the UK and Ireland (Shennan et al., 2018; Smith et al., 2019). With a focus on RSL change, the sampling design of many of the original studies targeted sites in relatively sheltered locations, seeking continuous records of sedimentation wherever possible. Nevertheless, a number report evidence of breaks in sedimentation, breakdown of coastal barriers or abrupt changes in sediment type. None of these were attributed to the Storegga tsunami in these publications, probably because during the early Holocene RSL was rising towards the mid-Holocene highstand in this region, which provides a compelling alternative explanation for these features (Shennan et al., 2018). Some studies, however, do note the Storegga tsunami as a potential alternative explanation of sedimentary evidence for a high-energy event, rather than a major storm surge (Shennan et al., 1999; Jordan et al., 2010; Selby & Smith, 2016). Today we have more precise age constraints on the Storegga tsunami, 8120–8175 BP, than previously available (Bondevik et al., 2012) and increasing resolution in numerical simulations of wave propagation (Hill et al., 2014; Long et al., 2016; Bateman et al., 2021). In this paper we evaluate new and existing stratigraphic data from this region and improve the resolution and geographical extent of tsunami wave propagation modelling in northwest Scotland to test the hypothesis that the Storegga tsunami did impact the northwest coast of Scotland.

In section 2 we describe the methodology used to re-evaluate existing stratigraphic and microfossil data, and new high-resolution tsunami modelling developed in this study which we use to test the hypothesis that sites in northwest Scotland were impacted by the Storegga tsunami.

In section 3 we assess the evidence from a previously published site, Gortenachullish (Fig. 1), where previous studies provide evidence of abrupt changes in sedimentation at the time of the Storegga tsunami and report new particle size data to further test the tsunami hypothesis.

In section 4 we evaluate tsunami model predictions against previously published evidence from other sites in this region which have sediments accumulating across the time of the tsunami and either have evidence of no tsunami sedimentation or evidence of changes that may possibly be related to a tsunami.

Broadly three different types of sites exist (Fig. 1): coastal wetlands behind a gravel or sand barrier; lake basins that at some point were connected to the sea and are now isolated from the sea and partly or fully infilled with sediment; and

*Correspondence: Sarah A. Woodroffe, as above.
E-mail: s.a.woodroffe@durham.ac.uk

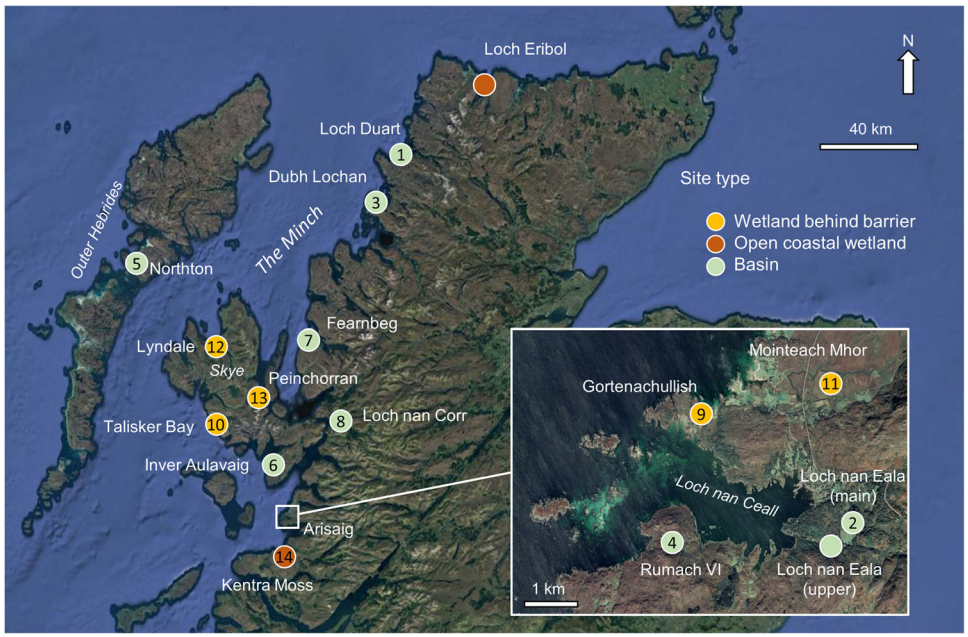

Figure 1. (A) Location of sites across northwest Scotland discussed in the text, inset: Arisaig area. Numbers refer to site labels on Figure 8. (*Source*: 'NW Scotland', centred on 56.58, −4.69. ©Google Earth. Landsat/Copernicus image taken on 14 February 2015 accessed on 10 October 2022). [Color figure can be viewed at wileyonlinelibrary.com]

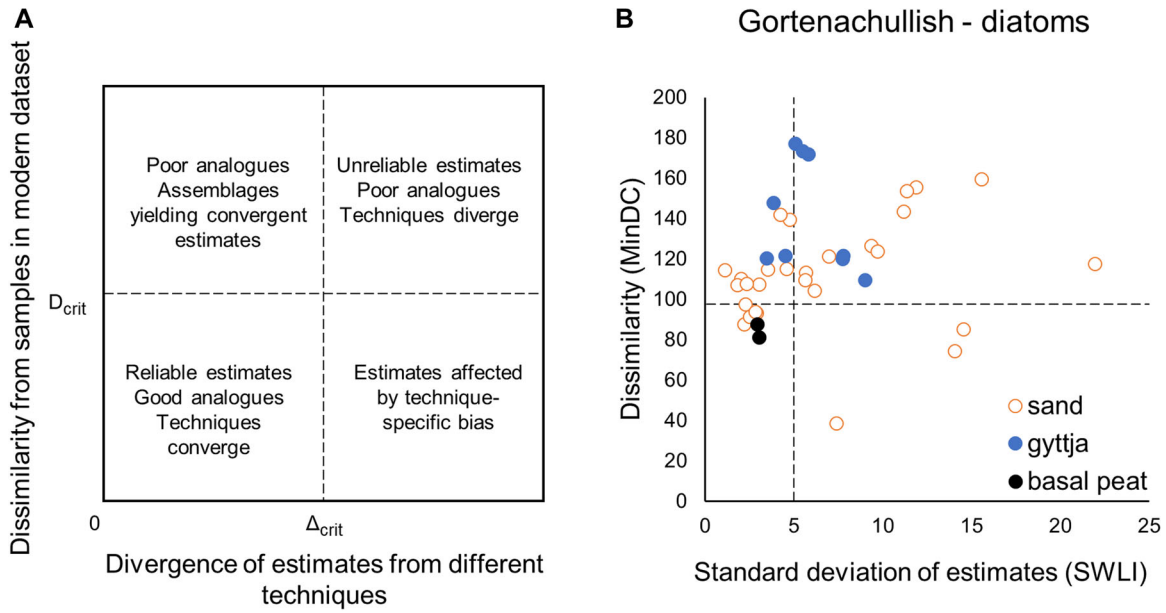

Figure 2. (A) Conceptual model for assessing the reliability of palaeoenvironmental reconstructions based on a scatterplot of dissimilarity *D* between the modern and fossil samples, against method divergence Δ (Kucera et al., 2005). For heterogeneous modern datasets (diatoms) the 5th percentile defines D_{crit} and for homogenous modern datasets (e.g. foraminifera) the 20th percentile (Kemp & Telford, 2015). For Δ_{crit} we use the standard deviation of six transfer function model estimates, when SD = 5 SWLI. (B) Goodness of fit for diatom assemblages at Gortenachullish. [Color figure can be viewed at wileyonlinelibrary.com]

coastal wetlands open to the sea. Each category has potentially different detection limits of palaeo-tsunamis. Coastal sediment sequences that produce identifiable palaeo-tsunami evidence depend upon two critical thresholds for each type of indicator: creation thresholds and detection thresholds. To exceed creation thresholds, palaeo-tsunami indicators must be distinct from similar indicators that may result from other processes, such as RSL change or coastal geomorphic processes. We consider creation and detection thresholds at each site in reference to five criteria diagnostic of abrupt changes in sedimentation at the time of the Storegga tsunami: (i) lateral continuity of the stratigraphic evidence between boreholes or outcrops; (ii) sediment deposit thins in a landward direction; (iii) a sharp contact between the sediment layers; (iv) a distinct change in sediment lithology and/or biostratigraphy; and (v) age control for the period when the Storegga slide occurred.

Methods

Sediment analysis at Gortenachullish

The site at Gortenachullish (numbered 9 on Fig. 1) was resampled in 2019 (GA19-1) within 10 m of the sampled core from Shennan et al. (1999) (GA95-1), to undertake detailed analysis of grain size that may indicate the mode of deposition

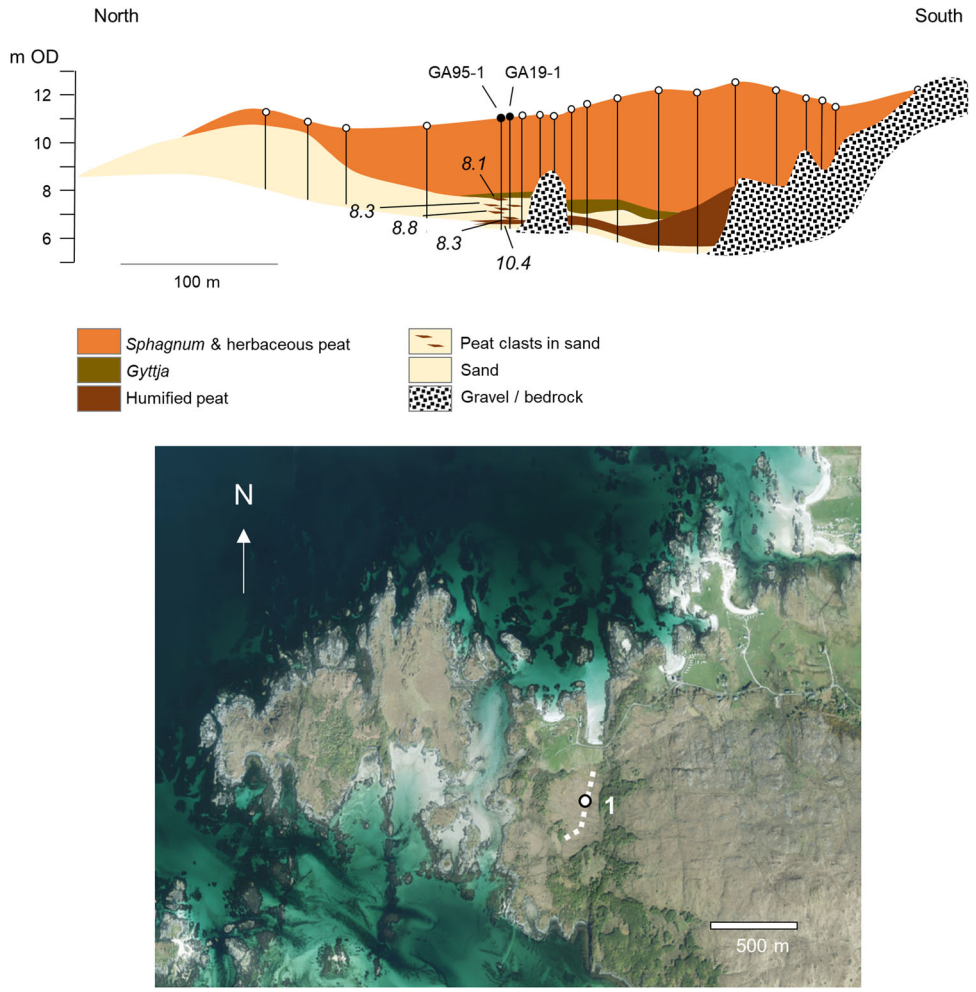

Figure 3. Stratigraphy of the peat bog at Gortenachullish showing locations and elevations (in metres Ordnance Datum, the UK vertical datum for reporting elevation) of cores taken in 1995 (white dots) and the location of GA19-1 which replicates the analysed core GA95-1 from Shennan et al. (1999). Ages are a summary of radiocarbon data from Table 1 indicating that the sand layer was deposited around the time of the Storegga tsunami. Also shown is a satellite image of the location of the original core transect (dashed line) and core sampled in 2019 (labelled 1). (*Source*: 'Gortenachullish', 56.9196, −5.8786. ©Google Earth. CNES/Airbus image taken on 29 August 2021 accessed on 10 October 2022). [Color figure can be viewed at wileyonlinelibrary.com]

of the sand layer. We sampled the site with a 50-mm-diameter piston corer to collect material for laboratory analysis. We undertook particle size analysis on the ~0.7-m-thick sandy section of core GA19-1 at 5-mm intervals using a Coulter laser particle size granulometer, after pretreatment with hydrogen peroxide to dissolve organic material. We analysed the data in GRADISTAT (Blott & Pye, 2001) to produce % frequencies of different size fractions on the Wentworth scale (e.g. % fine sand) and we calculated the mean particle size for each sample using the Folk and Ward (1957) method.

To further improve understanding of the environments immediately before and after the Storegga tsunami at Gortenachullish, we use a new diatom transfer function approach to aid our interpretation of this sediment sequence. Although diatoms and pollen were analysed from core GA95-1 at Gortenachullish in the original Shennan et al. (1999) study (see Figs. 3 and 4), their focus was not on reconstructing the environments immediately below and above the sand layer, and they did not use a transfer function approach to quantitatively reconstruct the elevation of these palaeo-environments.

The basic concept of the transfer function approach is to express the value of an environmental variable, sediment surface elevation relative to sea level, as a function of biological information, in this case, diatom assemblages. As part of this study we have assembled a new dataset of 469 modern diatom samples from around Great Britain, using published sources and from our unpublished work as the training set from which to quantitatively reconstruct the elevation of the different environments within the GA95-1 core (details in the Supporting Information). The newly assembled dataset includes samples from intertidal flats below mean tide level, through salt marsh environments, to freshwater wetlands above highest astronomical tides. To allow for differences in tidal range, we use standardized elevations, expressed as the Standardized Water Level Index (SWLI; Kemp & Telfer, 2015). In this method, 200 SWLI = mean high water of spring tides and 100 = mean tide level.

We follow the conceptual model of Kucera et al. (2005) for assessing the reliability of palaeoenvironmental reconstructions based on a scatterplot of dissimilarity D between the modern and fossil samples, against method divergence Δ (Fig. 2A). For heterogeneous modern datasets, such as diatoms, the 5th percentile defines D_{crit} (Kemp & Telford, 2015). For Δ_{crit} we use the standard deviation (SD) of model estimates of elevation from six different transfer functions, when 1 SD = 5 SWLI units. This simple method provides a tool that focuses attention on the interpretation of the differences between reconstructions

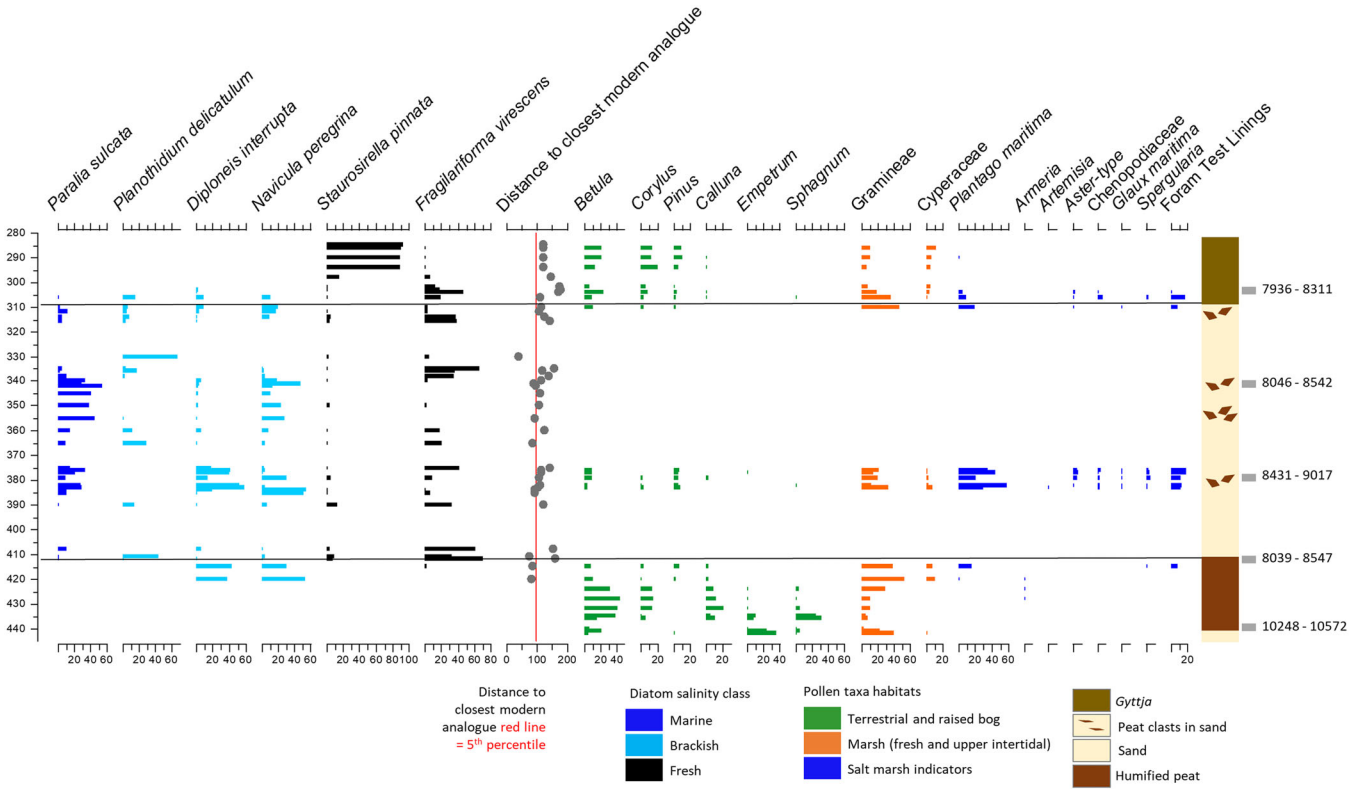

Figure 4. Gortenachullish microfossils from sediment core 95-1 – analyses using data from Shennan et al. (1999). ^{14}C ages are recalibrated using INTCAL20 in CALIB 8.2 (Stuiver & Reimer, 1993; Reimer et al., 2020). Also shown is the statistical-based interpretation of closeness to modern analogues (see Methods for details of the method used). [Color figure can be viewed at wileyonlinelibrary.com]

from different techniques. It can be used in a more formal approach by taking more than two methods and calculating the standard deviation of the different estimates (Juggins & Birks, 2012). Where different models produce consistent rather than conflicting reconstructions, these may be combined into a single, consensus reconstruction with the standard deviation between reconstructions as a measure of reliability (Juggins & Birks, 2012; Kemp & Telford, 2015).

We applied this approach to the Gortenahullish diatom data (Figs. 2B and 4). We trimmed the 469 modern samples to 427 by excluding those below 100 SWLI and above 300 SWLI, i.e. those from below mean tide level (MTL) and those higher than 2 m above mean high water of spring tides (MHWST). Model performance deteriorates at the upper and lower extremes of the full dataset. We created six transfer function models: Weighted Averaging Partial Least Squares; Locally Weighted Weighted Averaging Partial Least Squares (inverse deshrinking); Locally Weighted Weighted Averaging Partial Least Squares (classical deshrinking); Modern Analogue Technique; Modern Analogue Technique (weighted average); and Maximum Likelihood. Figure 2B shows that transfer-function-derived elevation estimates in the basal peat are reliable with good modern analogues, within the sand layer they are unreliable with divergent elevation estimates and within the overlying gyttja they are unreliable due largely to poor modern analogues. We use this information to improve understanding of environmental conditions before, during and after the sand deposition in the Results for Gortenachullish.

Information on the methods used to sample other sites described but not re-sampled in this study are found in the original publications and not repeated here. References to those studies appear where the sites are described in the Results.

Storegga tsunami modelling

To understand the potential of the Storegga tsunami wave to inundate sites along the NW coast of Scotland, we carried out a similar modelling strategy to Bateman et al. (2021) using a high-resolution Shallow Water Equation Solver, driven by the model of Hill et al. (2014) as boundary conditions. The flow model here is a 2D non-linear, non-conservative, Shallow Water Equation solver (*Thetis*; Kärnä et al., 2018) with wetting and drying (inundation) incorporated within it. The model uses realistic palaeobathymetry constructed from modern bathymetry which is corrected for glacial isostatic adjustment (GIA) (Bradley et al., 2011). However, this does not account for other changes in bathymetry due to reasons other than RSL change or the effects of tides. The modelled domain covers the whole region of interest using spatially varying model resolution. Resolution varies from 2.5 km to 30 m over the domain depending on water depth, distance from the boundary and proximity to areas of interest. Our original bathymetric data were at 50-m horizontal resolution across the whole domain, but 5-m horizontal resolution data are used at sites of interest (Intermap Technologies, 2007). The topographic data are blended together using HRDS (Hill, 2019). Wave height can be extracted from each site of interest (Fig. 1) via interpolation of the finite element function. *Thetis* calculates the water height and velocity of the flow even if the site is not underwater (for details see Kärnä et al., 2011). A detailed explanation of the modelling methodology is provided in the Supporting Information. To consider whether each site would have been inundated by the modelled Storegga tsunami, we consider the height of the modelled waves in metres Ordnance Datum (m OD) (including the modelled palaeo-spring tide range at each location to give an idea of tide-dependent inundation; Neill et al., 2010) against the elevation of organic sediment or

coastal barrier/sill at that location, which provide threshold elevations at each site.

Results

Gortenachullish

This site was first sampled in 1995 (Shennan et al., 1999), revealing a peat wetland behind a sand ridge, facing north (Fig. 3). At ~3.5–4 m depth there is a sand layer abruptly overlying a basal peat which thins landward, and has an eroded upper contact between the peat and the sand. Some of the cores taken in 1995 had clasts of peat present within the sand layer. The top of the sand is overlain by a gyttja that transitions upwards to a *Sphagnum* and herbaceous peat. Radiocarbon ages show the basal peat is from the early Holocene, with saltmarsh sediment immediately below the sand layer dated to 8.3k cal a BP (Table 1). The peat clasts found within the sand layer are of similar age to the upper part of the underlying peat (8.3 and 8.7k cal a BP), suggesting they were reworked from the underlying section and incorporated into the sand during rapid deposition (Fig. 3 and Table 1). The base of the gyttja above the sand is dated to ~8.1k cal a BP. The original publication suggests that the sand layer records a sudden event, such as a storm, during which intertidal sand was remobilized to inundate the developing saltmarsh following a period of fast RSL rise when coastal systems in this region reorganized to a new RSL baseline. It does not mention the potential for the sand to be deposited by the Storegga tsunami (Shennan et al., 1999). The radiocarbon ages constraining the sand layer at Gortenachullish are older than those which were available at that time for sites in northeast and east Scotland with sediment sequences attributed to Storegga (Dawson et al., 1988, 1990; Smith et al., 1985, 2004). Later in this section we consider the age correlation with the much improved age constraints on Storegga now available (Bondevik et al., 2012).

Microfossils from the basal peat indicate a gradual transition from freshwater wetland, with ground flora of heathland shrubs, *Calluna* and *Empetrum*, and *Sphagnum* bog, to tidal marsh, Gramineae, *Plantago maritima*, and especially brackish diatoms that live part of the time exposed to the air (*Diploneis interrupta*). The transfer function models indicate sediment accumulation immediately below the sand layer was at about MHWST and the assemblages have good modern analogues in the modern training set, with minimum Dissimilarity Coefficient (minDC) values below the 5th percentile (Kemp & Telford, 2015) (Fig. 4).

The sharp upper contact to the sand coincides with a marked change in diatom assemblages, with a change to a mix of marine, brackish and freshwater species. Pollen assemblages from one of the larger peat clasts are similar to the upper part of the basal peat (Fig. 4). The transfer function reconstructions are unreliable in this unit with divergent elevation estimates (Fig. 2B). At the top of the sand unit in core GA95-1 there is a change from sand with peat clasts, to sand–gyttja with organic fragments, to gyttja with no sand. Marine and brackish diatoms quickly disappear as the sand content decreases, along with salt marsh pollen indicators present in the basal peat and the peat clasts within the sand layer. The dominant diatom species in the sand-free gyttja is commonly associated with standing freshwater (*Staurosirella pinnata*). Samples from such environments are not well represented in the UK-wide modern coastal diatom training set and the minDC values indicate poorer modern analogues than in the organic unit below the sand, suggesting that this is not a saltmarsh environment (Fig. 4).

Our new analysis of the particle size distribution within the sand layer shows the lower 45 cm of the sand has relatively stable mean particle size and the upper 28 cm shows a fining-upwards sequence with increased percentage of fine sand and a decrease in mean particle size (Fig. 5A). Radiocarbon ages from the top of the peat immediately below the sand layer and the freshwater gyttja directly above the sand layer in the core from the Shennan et al. (1999) paper are entirely consistent with the hypothesis that the sand was deposited at the time of the Storegga tsunami in the form of a sandy tsunamite (Fig. 5B and Table 1).

The different lines of evidence, including sediment stratigraphy (sharp lower contact, gradational upper contact), evidence of a fining-up sequence in the upper part of the sand layer, the age of the deposit, its morphology of thinning landwards across the site and the microfossil evidence suggesting the sand is of marine origin, are all compatible with Gortenachullish recording the Storegga tsunami (Bondevik et al., 1997; Dawson & Shi, 2000; Smith et al., 2004; Chagué-Goff et al., 2011). The fining-up sequence is typical of suspension deposition and is a common feature of Storegga tsunami deposits from estuarine and bayhead environments in Scotland (Smith et al., 2004; Long et al., 2016). The microfossils are mixed assemblages, with sources ranging from marine water and sediments brought in by the tsunami, eroded salt-marsh deposits seen at the base of the sequence, and more landward sources eroded during wave backwash. We suggest that this site developed from a freshwater marsh into a saltmarsh environment in the early Holocene as local RSL rose (Fig. 6A), the Storegga tsunami hit, eroding the saltmarsh environment and depositing a 65- to 100-cm-thick sand layer and initiating a coastal barrier (Fig. 6B). Soon after, a freshwater lake formed behind this barrier (Fig. 6C) which accumulated to higher elevations during gradual RSL rise. The site eventually

Table 1. Radiocarbon dates from core GA95-1 from Gortenachullish, first reported in Shennan et al. (1999). ^{14}C ages are recalibrated using INTCAL20 within Calib 8.2 (Stuiver & Reimer, 1993; Reimer et al., 2020).

Laboratory code	Depth in core GA95-1 (m)	Altitude (m OD)	^{14}C a BP ± 1σ	Cal a BP ± 2σ	Mid cal age and range	Comment
UB-4031	302–304	7.99–7.97	7270 ± 80	7936–8311	8122 ± 180	Freshwater gyttja, directly above gyttja with sand and organic fragments, and ~6 cm above top of sand with peat clasts
UB-4032	340–342	7.61–7.59	7529 ± 98	8046–8542	8294 ± 248	Peat clast within the sand unit
UB-4033	376–378	7.25–7.23	7903 ± 118	8431–9017	8724 ± 293	Peat clast within the sand unit
UB-4034	411–413	6.90–6.88	7535 ± 109	8039–8547	8293 ± 254	Saltmarsh sediment immediately below the sand layer
UB-4035	439–441	6.62–6.60	9246 ± 67	10 248–10,572	10 410 ± 162	Freshwater peat at the base of the core

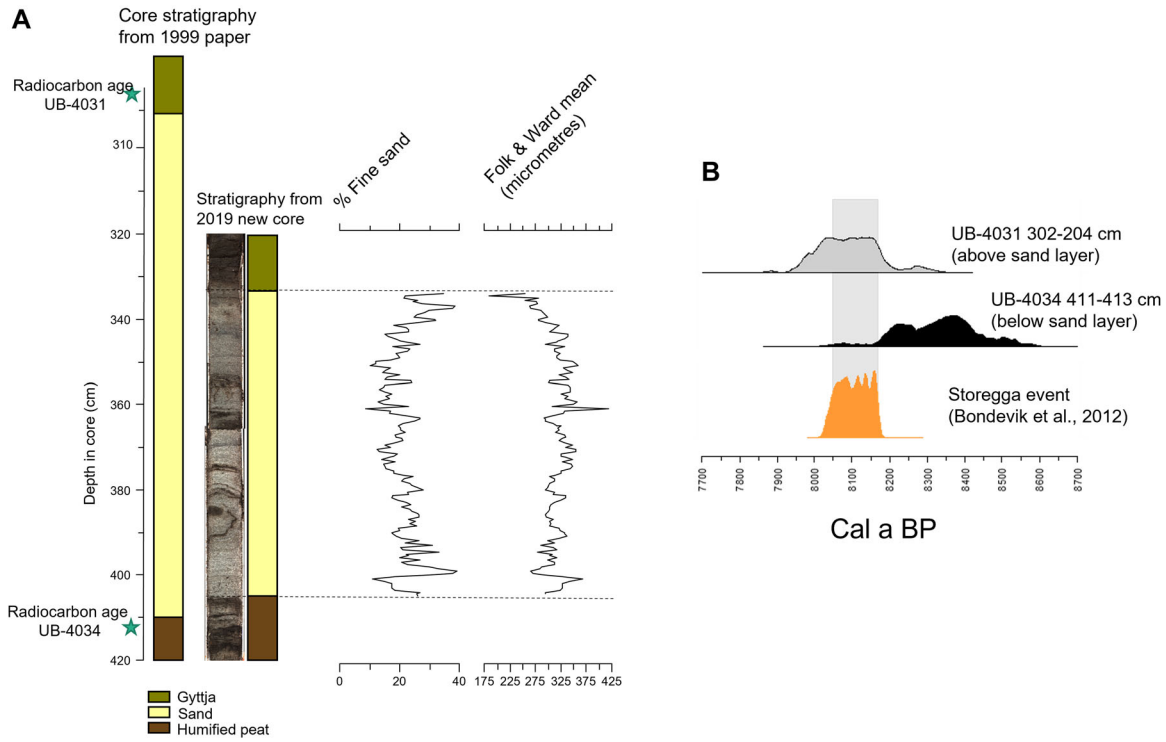

Figure 5. (A) New core photograph and particle size data from Gortenachullish core GA19-1, and the lithology log from core GA95-1 from Shennan et al. (1999) for reference. (B) Chronology of the bracketing dates, below and above the sand layer in the original core, GA95-1, and the age of the Storegga slide (Bondevik et al., 2012), all recalibrated using INTCAL20 in CALIB 8.2 (Stuiver & Reimer, 1993; Reimer et al., 2020). [Color figure can be viewed at wileyonlinelibrary.com]

developed into a raised bog that was not inundated by the local mid-Holocene RSL highstand (Fig. 6D).

We can estimate tsunami run-up based on the elevation of the sediment horizons below and above the sand layer, their ages and their reconstructed position in relation to RSL (^{14}C-dated horizons 8.3 and 8.1k cal a BP, at 6.9 and ~8 m OD, in saltmarsh immediately below the sand layer and freshwater gyttja 6 cm above the sand layer; Fig. 4, Table 1). At the time of the Storegga tsunami event, spring high tides were ~6.9 m OD, based on the saltmarsh environment at this elevation in the core immediately prior to the event. The fact that freshwater limnic sediment is deposited above the sand layer at ~8 m OD infers a wave-deposited sand barrier must have reached at least 8 m OD (core sample elevation), but was probably higher (~9 m OD) to create sufficient water depth to enable limnic sediments to be deposited behind it. Therefore the minimum wave run-up must have been ~2 m (6.9–9 m) but was possibly higher (up to ~6 m based on current tidal range in this region) depending on the stage of the tide when the tsunami hit.

Tsunami modelling results

The modelled tsunami wave reaches the northern edge of the simulation 3 h after the source initiation. All times described below refer to time from simulation which is tsunami initiation + 3 h. The tsunami has a complex form which develops due to the slow travel of the wave south of the Minch (Fig. 1) compared to the more rapid travel to the west of the Outer Hebrides (Fig. 7). Following the passing of the leading wave (~3 h into the simulation at the northerly edge of the region) a number of reflections develop from various inlets and areas of complex coastline causing localized peaks in wave height between 4 and 6 h into the simulation. Subsequent waves then travel south (~ 6 and ~9 h at the northern edge), following a similar pattern. The Isle of Skye forms a blockage to waves travelling south, such that waves travelling down the west coast of the mainland are effectively blocked, but the wave refracts around the western coast of Skye (e.g. at 5 h in Fig. 7). In addition, the wave travelling south to the west of the Outer Hebrides turns northward (e.g. at 11 h, after the third wave in Fig. 7). The area south of Skye therefore has a complex set of waves impacting the coastline, both from the immediate north around the west of Skye, but also from the south due to refraction from the west of the Outer Hebrides.

Plotting the wave heights and extracted topographic height for all sites shows a mix of inundation around the simulation, which also depends in some instances on the phase of the tide at the time the waves pass (Fig. 8). The Storegga tsunami creates unusually high waves at all sites, with the effect ongoing at least 12 h into the simulation (15 h after initiation of the tsunami). For the more northerly sites (Loch Duart Marsh and Dubh Lochan) there are several peaks and troughs during the simulation, whereas for the more southerly sites there are three distinct peaks in wave height, ~5, 7 and 9–10 h into the simulation. Several sites have barriers or sills that are very close to the maximum wave height so the tidal height between 3 and 11 h is an important factor in whether they are inundated or not. Maximum wave height at the sites in this study during the simulation varies between 2.7 and 9.4 m above contemporaneous mean tide level (Fig. 8), but the potential for inundation is heavily influenced by the geomorphology of the site and the tidal height when each wave hit. Tsunami modelling clearly shows that the northwest coast of Scotland was affected by the Storegga tsunami, and that there is potential for existing sites in this region to have a sedimentary record of it.

Discussion

In this section we evaluate tsunami model predictions against the sedimentary indicators at different locations in the region

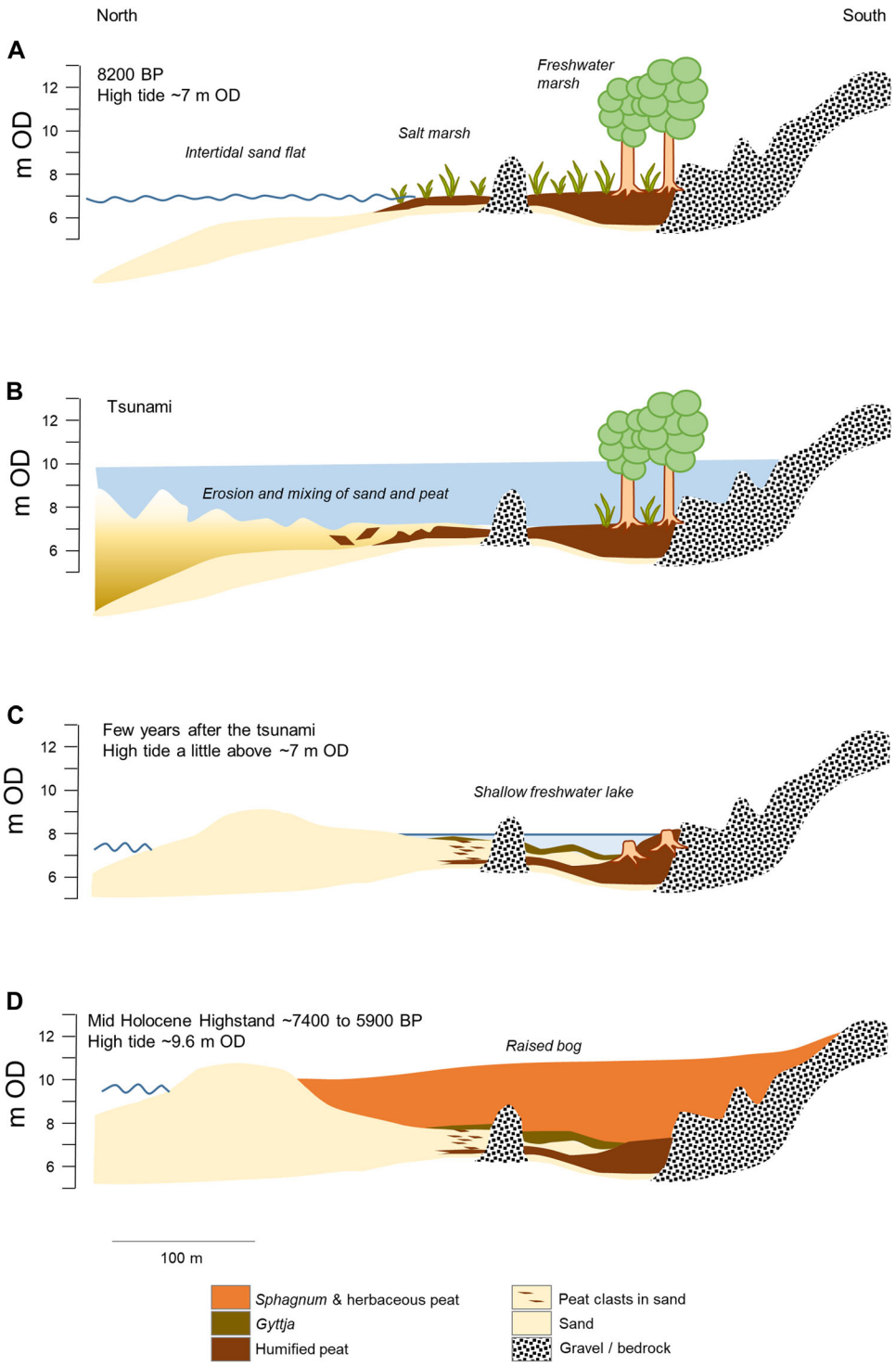

Figure 6. Model of site evolution at Gortenachullish between the time immediately before the Storegga tsunami (A), during the tsunami (B), after the tsunami (C), and the later mid-Holocene RSL highstand (D). This figure has the same profile as in Figure 3 with a N–S orientation from left to right across the page. In C 'a few years after the tsunami' indicates when sufficient time had passed for deposition of organic gyttja on top of the tsunami-deposited sand (light brown horizon in C). D represents the theoretical situation at the mid-Holocene highstand (7.4–5.9 ka) when RSL was ~9 m above present. The present-day situation depicted in Figure 3 deviates from this as RSL has since fallen and the sphagnum and herbaceous peat unit has prograded over the sand barrier to the north of the site. [Color figure can be viewed at wileyonlinelibrary.com]

(Fig. 8). The sedimentary evidence around the time of the Storegga event comes from a range of different coastal settings, primarily coastal wetlands behind a gravel or sand barrier: lake basins that at some point were connected to the sea and are now partly or fully infilled with sediment and coastal wetlands open to the sea. The ability of each coastal setting to record the Storegga tsunami depends on the local availability of sediment to be deposited, the elevation of coastal barriers impeding wave ingress and the type of existing environment which might be more or less sensitive to recording marine inundation in sediments and/or microfossils (Bondevik et al., 1997).

At the time of the Storegga event, all of the sites were experiencing RSL rise, at different rates, reflecting the balance between global, barystatic sea-level rise and spatially variable GIA (Fig. 9) (Bradley et al., 2011; Shennan et al., 2018). RSL rise frequently promotes landward migration of coastal sedimentary systems, depending on local factors such as sediment supply and

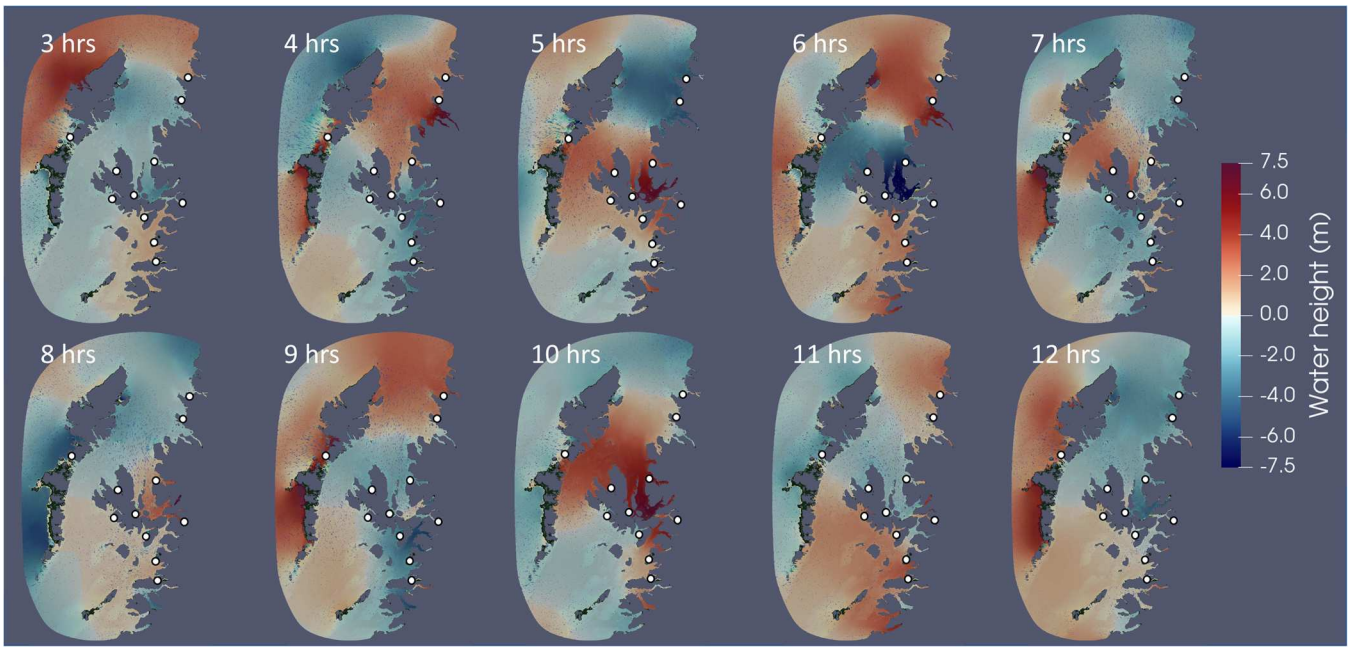

Figure 7. Wave heights at hourly intervals between 3 and 12 h into the simulation. The study locations are indicated by white dots. [Color figure can be viewed at wileyonlinelibrary.com]

accommodation space. We evaluate whether the palaeotsunami indicators at each site are distinct from similar indicators that may result from other drivers, such as RSL change and coastal geomorphic processes.

Barrier wetland sites

Gortenachullish, described in the Results, is a wetland site behind a barrier at present but at the time of the Storegga event the sediment lithology and the pollen and diatom evidence reflect a tidal salt marsh, with daily tidal inundation indicated by the dominant diatom species, forming at approximately high spring tides. The marsh may have been protected by a barrier across part of the site entrance but not sufficiently extensive to prevent tidal inundation. The elevation of high spring tides fits well with the tsunami model predictions (Fig. 8B), both for RSL at model-time zero, the peat elevation occurring at the top of the tidal range, and for inundation by the tsunami. The tsunami model predicts potentially multiple waves up to 2 m above the peat elevation that could deposit the sand layer. The waves would not reach the site if the phase of the tide was below mean tide when the waves passed.

The other barrier wetland sites (Mointeach Mhor, Peinchorran, Lyndale and Talisker Bay) differ from Gortenachullish in that their sediment lithologies and biostratigraphies immediately prior to the time of the Storegga event do not indicate salt marsh and active tidal fluctuations with the open sea.

Mointeach Mhor, close to Gortenachullish (Fig. 1), was a freshwater wetland with peat accumulation at the time of the Storegga event (Shennan et al., 1995a, 2005) and was not inundated until ~7.5k cal a BP. Peat formed in this wetland at the same elevation as RSL at the time of the Storegga event so it must have been protected by a barrier. The barrier crest elevation in Figure 8 is that for the fossil barrier, described in previous accounts, which excluded marine sediments from the site until ~7.5k cal a BP. We do not know the precise elevation of the barrier crest at the time of the Storegga event but it must have been sufficient to protect the site from the predicted tsunami waves (Fig. 8B).

The barrier sites on Skye (Fig. 1), namely Peinchorran, Lyndale and Talisker Bay, record clastic sediment accumulation at the time of the Storegga event, with diatom assemblages recording water salinity in these back-barrier settings. The three sites present different scenarios with respect to the tsunami model predictions. Peinchorran on the east coast of Skye is a former lagoon and peatland behind a double tombolo of sand and gravel ridges (Selby & Smith, 2007, 2016). Diatom assemblages record changes in water salinity in a lagoon environment from *c.* 8.8 to 4.4k cal a BP. The authors identify no washover sediments and suggest there was no direct connection to the sea during this time-period. At the time of the Storegga event the lagoon sediment was an organic silt dominated by polyhalobous diatoms. Modelling suggests that this silt (~4.3 m OD) and both barriers (~7–8.3 m OD) would have been overtopped by tsunami waves, with a run-up up to ~4 m above the height of the barriers (Fig. 8B), or more if the tsunami hit at high tide. Although the Storegga tsunami is modelled as a significant event to hit Peinchorran, the creation threshold seemingly was not passed as no sand or gravel layer is recorded. The sediments were already dominated by polyhalobian diatoms and therefore sudden marine inundation is undetectable in the biostratigraphy.

Lyndale, on the north coast of Skye, has a sequence of basal gravel overlain by silt and then peat behind a gravel barrier at 5.6–6.8 m OD (Selby & Smith, 2016). In one core the basal sediments consist of gravel overlain by 0.2 m of peat and sand which turns into silt up core. Seven centimetres below the top of the peat–sand is dated to 8199–8381 cal a BP (7497 ± 32 ^{14}C a BP) (Selby & Smith 2016, Figs. 5 and 6 and age recalibrated using INTCAL20). There is a rise in marine and brackish diatoms between the peat–sand and the overlying silt. The original interpretation was of sediments accumulating during a continuous rise in RSL in a quiet water environment behind a barrier (Selby & Smith, 2016), and even though the barrier crest may have been lower than at present, this interpretation does not conflict with the predicted tsunami not overtopping the barrier (Fig. 8B).

At Talisker Bay there is a buried organic silt but unlike the other sites it has a gravel horizon dated to around the time of the Storegga event (Selby & Smith, 2016; Smith et al., 2019). Tsunami modelling indicates wave heights just below the lowest of the multiple barrier crests in Talisker Bay (Fig. 8B).

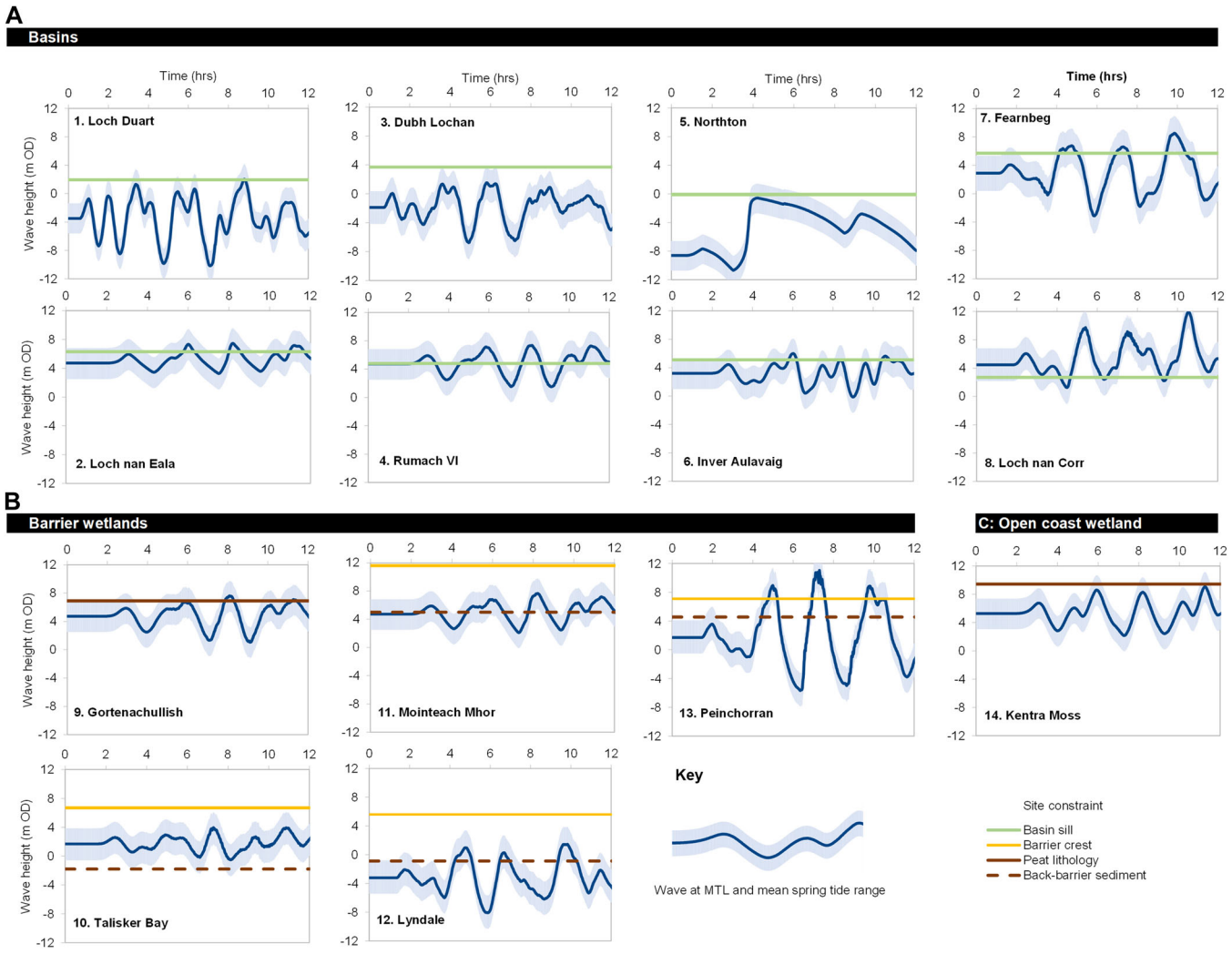

Figure 8. Tsunami model predictions of wave height scaled to metres OD. Model-time zero is Storegga slide initiation +3 h as there are no waves in this region until this time. Blue line shows wave height when the phase of the tide is at mean tide level, so in ~6.1 h the tsunami wave would change from occurring around high tide to low tide, with the range illustrated in light blue. The range shows present-day mean spring tide range, whereas Neill et al. (2010) suggest tidal range was ~16% greater at the time of the Storegga event. The dark blue line at model-time zero indicates RSL at 8.15k cal a BP predicted by the GIA model used in the study. This could provide an additional offset in elevation depending on the fit of the GIA model with sea-level index points at each location (see Shennan et al., 2018). Site numbers refer to numbers on Figure 1. [Color figure can be viewed at wileyonlinelibrary.com]

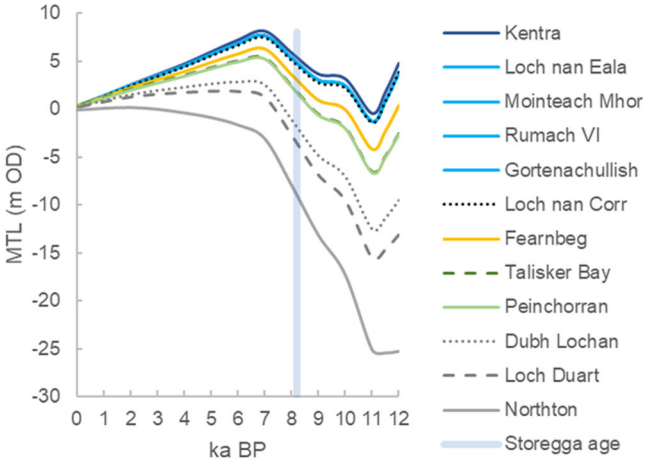

Figure 9. RSL through the Holocene at sites mentioned in the Discussion, predicted by the BRADLEY2011 GIA model (Bradley et al., 2011; Shennan et al., 2018). MTL (m OD) refers to mean tide level in metres in relation to Ordnance Datum, the UK vertical datum for reporting elevation. [Color figure can be viewed at wileyonlinelibrary.com]

At present, given the different heights of the Talisker Bay barriers it is not possible to definitively attribute the buried gravel horizon to the Storegga tsunami. To categorically rule this in or out it would be useful to reconstruct the evolution of the coastal barriers here.

Basin sites

Basins which were freshwater lakes and record marine ingression at the time of the Storegga event

Dubh Lochan is an isolation basin with marine sand overlying eroded freshwater gyttja indicative of sea-level rise. This is a key site because the basin sill was close to but just above high tide level at the time of the Storegga event. Dubh Lochan occupies a small embayment on the east side of Achnahaird Bay, ~130 km north of Arisaig and 60 km south of Loch Eribol (Fig. 1). The lake discharges into the bay via a stream that cuts through a small, vegetated gravel ridge down to a rock sill visible at 3.69 m OD (Shennan et al., 2000). The original paper shows a series of hand-driven cores revealing a basin behind the rock sill. In the deepest part of the basin the sediment

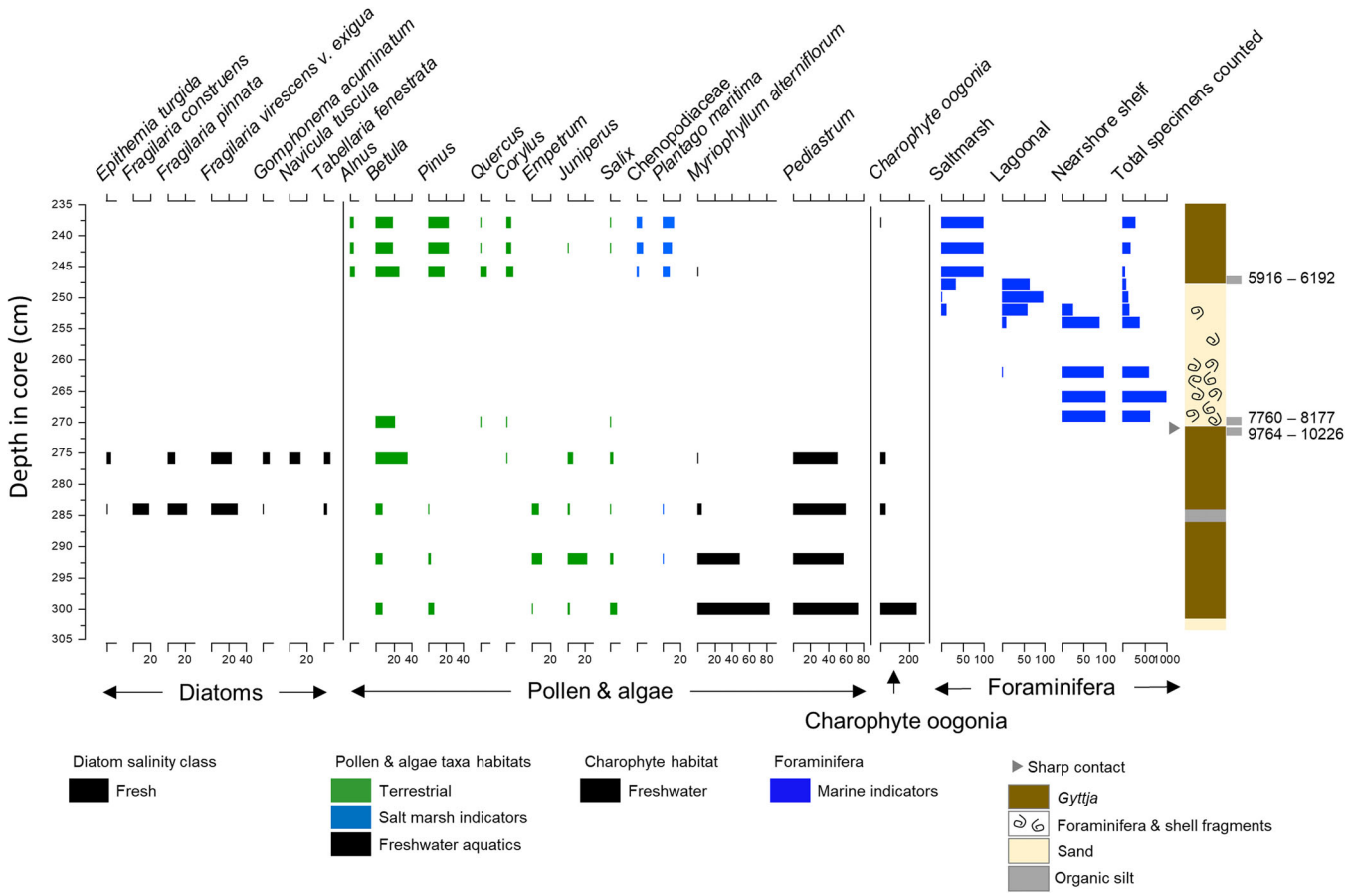

Figure 10. Dubh Lochan microfossils; data taken from Shennan et al. (2000) with previously unpublished diatom data. Diatoms shown as % total diatoms, pollen & algae as % total pollen, charophyte oogonia as raw counts, and foraminifera as % and total count. ^{14}C ages are recalibrated using INTCAL20 or MARINE20 (*) in CALIB 8.2 (Stuiver & Reimer, 1993; Heaton et al., 2020; Reimer et al., 2020). The marine date is calibrated using a ΔR of −111 ± 50 calculated from the mean of the six nearest marine reservoir ages (within 42 km of Dubh Lochan) taken from the Marine Reservoir Correction database (Harkness, 1983; Reimer & Reimer, 2001; Cappelli & Austin, 2020). [Color figure can be viewed at wileyonlinelibrary.com]

sequence comprises a basal sand then a lower gyttja with a 2-cm intercalated organic silt horizon within it (Fig. 10). A sharp contact occurs between the top of the gyttja and the overlying sand. This sand has abundant gastropods and foraminifera. The sand transitions upwards to a brown gyttja and then an herbaceous surface peat (Fig. 10).

The lower part of the sequence records Lateglacial and early Holocene environmental changes. Pollen, foraminifera and charophyte assemblages record the chronological sequence of environmental changes from that time onwards. Above the unfossiliferous basal sand the lower limnic unit contains freshwater microfossils, notably *Pediastrum*, *Myriophyllum alterniflorum* and charophyte oogonia. The changes in *Betula*, Cyperaceae, *Empetrum* and *Juniperus* pollen suggest that the intercalated organic silt represents the Younger Dryas Stadial.

The top of the lower gyttja, with an abrupt upper contact in all cores in which it is overlain by grey sand, has diatom and pollen assemblages indicating a freshwater lake environment. In contrast, the overlying sand contains a rich assemblage of gastropods and calcareous foraminifera, particularly *Cibicides lobatulus*. Recalibrated radiocarbon ages from the top of the gyttja (9764–10 226 cal a BP) and the foraminifera in the basal 1 cm of the sand (7760–8177 cal a BP) indicate a hiatus. In the original paper these data were interpreted as indicating rapid inundation of a freshwater lochan by marine water and erosion of the upper part of the freshwater gyttja, potentially caused by construction of a gravel barrier under conditions of RSL rise which was breached between 8.1 and 8.4 a BP. The original paper did not mention the potential for the gravel barrier breach to be caused by the Storegga tsunami (Shennan et al., 2000). The date on the foraminifera within the sand (7760–8177 cal a BP) is compatible with deposition at the same time as the Storegga tsunami, but the foraminifera only provide a maximum age for the sand, which may have been deposited later but contains older, reworked foraminifera (Fig. 10). A date from the gyttja above the sand layer is much younger (5916–6192 cal a BP, Fig. 10), thus providing a longer window of possibility for deposition of the sand layer than at Gortenachullish, for instance. RSL regression was underway in the basin by ~6.0k cal a BP (Fig. 10) and continued until ~4.8k cal a BP when the basin was isolated from tidal input across the sill (Shennan et al., 2000).

With the available evidence we cannot rule out that the gravel barrier breach and erosion of the sediments behind it was caused by the Storegga event, although we acknowledge that we cannot pin the age of the event conclusively to the time of the tsunami.

Shennan et al. (2000) suggested that a barrier-breach during rising RSL in the early to mid-Holocene might have caused the eroded contact. It is unlikely that the positive RSL tendency also happening at that time would have caused the erosional contact without an accompanying high-energy event (Bondevik et al., 1998). The Bradley et al. (2011) GIA model predictions of RSL at the time of the Storegga event lie ~2.5 m below the reconstructions of RSL based on field evidence (Shennan et al., 2018). Since the GIA-predicted RSL is used to define the tsunami elevation at model-time zero in Figure 8 (because the model uses GIA-predicted RSL to infer shoreline locations at the time of the Storegga event), the ~2.5-m discrepancy between the RSL predictions and reconstructions

would raise the tsunami-predicted heights by the same amount, and potentially allow multiple waves into the basin.

A similar situation exists at Loch Duart (Fig. 1) which would also have been a freshwater lake close to high tide level at the time of the Storegga event. The sedimentary evidence here suggests a marine incursion after ~10k cal a BP, which Hamilton et al. (2015) suggest was caused by marine transgression into the basin as RSL rose towards the mid-Holocene highstand. The ~10ka age comes from the upper contact of a freshwater unit that ends with an abrupt change in diatom assemblages, from freshwater to a mixed marine and freshwater flora. There are hardly any species common to the samples immediately either side of the contact. It is not stated whether the sediment lithology also shows an abrupt contact. Without further dating control it is not possible to say whether the abrupt change in diatom stratigraphy represents a hiatus, so the date of 10k cal a BP represents a maximum age for inundation of the basin.

The basin at Northton on Harris (Fig. 1) also records rapid marine inundation around the time of the Storegga event when RSL was ~8 m below the elevation of the basin sill (sill height 0.08 m OD; Jordan et al., 2010) (Fig. 8A). A rapid change from peat with freshwater diatoms to sand with marine diatoms invokes run-up of ~8 m as the tsunami wave travelled rapidly along the western coast of the Outer Hebrides (Figs. 7 and 8A). This fits with the tsunami wave height predicted in this study (Fig. 8).

Fearnbeg (Fig. 1) would also have been a freshwater basin close to high tide level at the time of the Storegga event (Shennan et al., 1996) or may already have infilled and become a terrestrial peat bog. Although this basin was cored for sea-level reconstruction, the original study focused on the deeper part of the sequence which records basin isolation in the Lateglacial period. The Younger Dryas and Holocene sediments were not analysed in detail, and therefore evidence here for the Storegga tsunami may have been missed. The model results suggest that this basin would probably have been inundated by the passing Storegga tsunami waves.

Basins with active connection to the sea at the time of the Storegga event

Other basins, namely Loch nan Eala (main and upper basins), Rumach VI, Inver Aulavaig and Loch nan Corr, had active connection to the sea at the time of the Storegga event. The sills of Loch nan Eala (main and upper basins), Rumach VI and Inver Aulavaig were in the upper part of the intertidal zone at the time of the Storegga tsunami and are modelled to have been inundated (Fig. 8A). The stratigraphies cored from the centre of Loch nan Eala (main and upper basins) and Rumach VI do not record any erosional contacts or sand layers and indicate marine diatoms during this time as would be expected from their sill elevations (Selby & Smith, 2016, 2007; Shennan et al., 2018, 2000, 1999, 1994). It is possible that sand layers may be preserved nearer to the sills of these basins which were not targeted by the original studies, or that conversely no sediment deposition occurred due to the Storegga tsunami. In particular, a shelly gravel layer near the sill of Rumach VI was hard to core through and not dated in the original study (Shennan et al., 1999).

Inver Aulavaig, an isolation basin in southern Skye, records gradual RSL changes between *c.* 15 and 3k cal a BP, although hard water effects from the limestone catchment may affect the older part of the record (Selby et al., 2000; Selby & Smith, 2007, 2016). The later sediments record early Holocene RSL rise into the basin, with clastic sedimentation and broad assemblages of marine, brackish and freshwater diatoms, through to late Holocene RSL fall, isolation from the sea and organic sedimentation. A few boreholes across the basin have a coarser layer within the Holocene clastic unit. In the deepest core sampled for radiocarbon and microfossil analysis, a 0.18-m-thick brown–grey silt with sand and gravel coincides with a rapid increase in marine diatoms, and a 1-cm-thick bulk sediment sample was dated to 7963–9076 cal a BP (7640 ± 240 ^{14}C BP) (Selby et al., 2000; Selby & Smith, 2007, 2016; and age recalibrated using INTCAL20). The authors do not suggest a correlation with the Storegga event, but further sampling at the site, with particular focus on providing a more precise chronology, is required to determine if this silt–sand–gravel is a record of the tsunami.

Loch nan Corr, at the head of Loch Duich (Lloyd, 2000; Lloyd & Evans, 2002; Shennan & Woodroffe, 2003) (Fig. 1), is predicted to experience significant wave heights as the southerly travelling waves blocked by the Isle of Skye are focused towards the Inner Sound between southern Skye, the mainland just north of Kyle of Lochalsh and the Applecross Peninsula (Figs. 7 and 8A). Our model predicts three very large waves, in the order of 7–10 m above the sill elevation (Fig. 8A). The basin was fully marine at the time of the Storegga event and therefore its creation and detection potential is dependent on the availability of sediment to enter the basin across the sill. The present outflow of the loch is along a small boulder-choked stream, ~200 m long. The sedimentary evidence suggests that at the time of the Storegga event the basin was surrounded by saltmarsh, with lagoonal sediments in the deeper parts, and ~6 m water depth. There is no obvious change in sediment lithology around the time of the Storegga event but there is a dramatic change in foraminifera, with an increase in species preferring fully marine conditions (Lloyd, 2000). This was dated by two samples, 7961–8180 cal a BP (7250 ± 60 ^{14}C BP) from bulk organic sediment and 8014–8177 cal a BP (7280 ± 40 ^{14}C BP) from the foraminiferal species *Cibicides lobatulus* (Lloyd, 2000, and ages recalibrated using INTCAL20). We hypothesize that the tsunami waves may have reconfigured the morphology of the connection between the basin and Loch Duich, for example by moving boulders, allowing a greater influx of marine water into the basin. Afterwards, more gradual coastal processes continued and the water salinity in the basin reflected the combined effects of gradual RSL change and movement of sediment into the 200-m stream course across the sill.

Open coast wetland

Two locations in the region previously analysed for RSL that have an open coastal configuration are Loch Eribol (Fig. 1), with Storegga tsunami deposits previously reported (Long et al., 2016), and Kentra Moss, which is a large outwash fan (*c.* 2 × 3 km) covered in peat, situated ~18 km south of Arisaig (Shennan et al., 1995b). The surface of the outwash slopes from the Loch Lomond Stadial ice-contact at Acharacle westwards to Kentra Bay, grading to a contemporaneous sea level at or below present. Peat accumulation on the surface of the outwash started ~9.3k cal a BP at 9.45 m OD, with no minerogenic sedimentation recorded in the peat. There is no visible evidence of sedimentation related to the Storegga tsunami here, only evidence to limit the maximum elevation of any predicted tsunami sedimentation to <~9.45 m OD (~4 m above RSL at the time of inundation) (Fig. 8C). Modelling suggests that the tsunami waves would only have reached the freshwater peat surface if they passed at high tide (Fig. 8C).

Conclusions

The Storegga slide and resultant tsunami was a significant event between 8120–8175 BP that impacted both the north and northwest coast of Scotland. The numerical model predicts run-up of between ~2.7 and 9.4 m above contemporaneous mean tide level at the sites analysed, with the highest on the west coast of the Outer Hebrides (Northton – 7.6 m), on the east coast of Skye (Peinchorran – 9.4 m) and at the head of long sea lochs such as Loch Duich (Loch nan Corr – 6.6 m). The tsunami is experienced differently at different locations, with those more northerly on the mainland experiencing multiple waves (e.g. Loch Duart and Dubh Lochan) whilst other sites experienced three or four main waves between 6 and 15 h post-initiation of the tsunami offshore Central Norway. The refraction of waves around Skye and the Outer Hebrides makes for a complex sequence of waves, but the model predicts that at least as far south as Mull on the west coast experienced significant wave heights (Fig. 7). The height and phase of the tide at the time of the initiation of the tsunami makes a difference to whether individual sites were inundated, because the tsunami waves took more than 8 h to arrive at different parts of the coastline (Figs. 7 and 8). There is scope to include tidal height and phase in a future modelling exercise to more accurately predict inundation potential through the tidal cycle.

The most compelling evidence for the Storegga tsunami is from Gortenachullish, which has a 0.65- to 1-m-thick sand unit with rip-up clasts on top of a saltmarsh peat. New particle size analysis backs up this interpretation with a fining-upwards sequence in the top ~25 cm of the sand and other criteria met including eroded lower contact, gradational upper contact, sand body fining landwards across the site, and microfossil and dating evidence (Bondevik et al., 1997; Smith et al., 2004). The morphology and elevation of the site along with local sediment availability means creation and detection thresholds are passed, and the modelling suggests the site would have been inundated if the waves passed between mean tide and high tide. By contrast, detecting the Storegga tsunami in isolation basins depends on the elevation of the sill at the time of inundation, its morphology and local sediment supply (Bondevik et al., 1997). A sill elevation just above highest tide level potentially produces the clearest evidence, e.g. Dubh Lochan and Loch Duart, but it is much harder to detect evidence in basins with sills which were low in the intertidal zone and there is likely to have been no change in sediment lithology (e.g. Loch nan Corr, Loch nan Eala, Rumach VI). Similarly, barrier locations with low intertidal sediments behind them rarely pass detection thresholds and it is impossible to determine the extent and elevation of barriers in the past (e.g. Lyndale, Talisker Bay). The open coast wetland at Kentra Moss would be a good test of creation and detection thresholds, but there is no visible evidence of minerogenic sedimentation related to the Storegga tsunami at this site. Erosion of a peat moss and a hiatus in the peat profile could be a new research target to further confirm the effects of the Storegga event in this region. Lastly, RSL was rising during the early Holocene at all studied locations and therefore evidence of rapid inundation sits within evidence for ongoing RSL rise, as is also the case at classic Storegga sites in Norway (Bondevik et al., 1998, 1997).

The predictions of wave height and inundation produced by the tsunami modelling provide a plausible explanation for the range of evidence of erosion, deposition or no change around 8150 cal a BP at the sites across northwest Scotland analysed in this study. Locations where field evidence indicate erosion or deposition due to the Storegga tsunami, where in the past this possibility has been dismissed or not considered, are predicted to be inundated by the modelling and therefore do not reject this alternative hypothesis, e.g. Gortenachullish, Dubh Lochan, Loch Duart, Inver Aulavaig and Loch nan Corr. Other sites predicted to experience significant wave heights (e.g. Peinchorran) where no evidence has been found may be because creation and preservation thresholds were not met due to their depositional environments (barrier location, basin with sill low in the intertidal zone), sediment availability or even the sampling strategy of the original study. A lack of evidence at other sites (e.g. Loch nan Eala, Rumach VI, Fearnbeg) which are predicted to be inundated but with less significant wave heights may be because the sampling strategy for the previous studies did not focus on collecting evidence to test the Storegga tsunami hypothesis.

Future field research to test the conclusions drawn here could, in addition to revisiting those sites noted above with a different sampling strategy, also focus on the area between Applecross and Skye where there should be open coast wetlands that may preserve evidence of erosion and/or deposition caused by the tsunami. Equally, the modelling suggests significant waves travelled as far south as Mull and therefore locations in the southwest highlands and Argyll and Bute should not be dismissed as unlikely to record the effects of the Storegga tsunami.

Supporting information

Additional supporting information can be found in the online version of this article.

Table A1. List of sites of interest

Figure A1. Areas of higher resolution topographic data (5 m horizontal resolution) are highlighted in darker shading on the background of lighter shading (50 m horizontal resolution). The areas of higher topography are around the sites of Peinchorran, Loch nan Corr and also around the four sites near Gortenachullish (Mointeach Mhor, Rumach VI and Loch nan Eala). The black line shows the 10 m contour used as a modelling boundary.

Figure A2. The simulated domain with forced boundary (red) and landward boundary (black). Sites of interested are named and listed in Table A1

Figure A3. View of the domain (A), with close up to show the changes in mesh resolution (red square). B) shows the wider area around Gortenachullish, with the red shaded box showing the area covered by C). Map C) shows the high resolution area, with mesh resolution at ~30 m in this area. The black line in all maps shows the 10 m contour used as a model boundary.

Acknowledgements. We acknowledge the GIA model output provided by Sarah Bradley which was used in the tsunami modelling. This project was undertaken on the Viking Cluster, which is a high-performance computing facility provided by the University of York. We are grateful for computational support from the University of York High Performance Computing service, Viking and the Research Computing team. Natasha Barlow, Ed Garrett and Roland Gehrels provided information for the modern diatom database. We acknowledge the careful and thorough reviews by Stéphanie Girardclos and Stein Bondevik which greatly improved a previous version of the manuscript.

Data availability statement

The data that support the findings of this study are available from the corresponding author upon reasonable request.

Abbreviations. BP, before present (1950 CE); GIA, glacial isostatic adjustment; MHWST, mean high water of spring tides; MTL, mean tide level; OD, Ordnance Datum; RSL, relative sea level.

References

Bateman, M.D., Kinnaird, T.C., Hill, J., Ashurst, R.A., Mohan, J., Bateman, R.B.I. et al. (2021) Detailing the impact of the Storegga Tsunami at Montrose, Scotland. *Boreas*, 50, 1059–1078. Available at: https://doi.org/10.1111/bor.12532

Blott, S.J. & Pye, K. (2001) GRADISTAT: a grain size distribution and statistics package for the analysis of unconsolidated sediments. *Earth Surface Processes and Landforms*, 26, 1237–1248. Available at: https://doi.org/10.1002/esp.261

Bondevik, S., Inge Svendsen, J. & Mangerud, J. (1997) Tsunami sedimentary facies deposited by the Storegga tsunami in shallow marine basins and coastal lakes, western Norway. *Sedimentology*, 44, 1115–1131. Available at: https://doi.org/10.1046/j.1365-3091.1997.d01-63.x

Bondevik, S., Løvholt, F., Harbitz, C., Mangerud, J., Dawson, A. & Inge Svendsen, J. (2005) The Storegga Slide tsunami—comparing field observations with numerical simulations. *Marine and Petroleum Geology*, 22, 195–208. Available at: https://doi.org/10.1016/j.marpetgeo.2004.10.003

Bondevik, S., Stormo, S.K. & Skjerdal, G. (2012) Green mosses date the Storegga tsunami to the chilliest decades of the 8.2 ka cold event. *Quaternary Science Reviews*, 45, 1–6. Available at: https://doi.org/10.1016/j.quascirev.2012.04.020

Bondevik, S., Svendsen, J.I. & Mangerud, J. (1998) Distinction between the Storegga tsunami and the holocene marine transgression in coastal basin deposits of western Norway. *Journal of Quaternary Science*, 13, 529–537. Available at: https://doi.org/10.1002/(SICI)1099-1417(1998110)13:6<529::AID-JQS388>3.0.CO;2-1

Bradley, S.L., Milne, G.A., Shennan, I. & Edwards, R. (2011) An improved Glacial Isostatic Adjustment model for the British Isles. *Journal of Quaternary Science*, 26, 541–552. Available at: https://doi.org/10.1002/Jqs.1481

Chagué-Goff, C., Schneider, J.-L., Goff, J.R., Dominey-Howes, D. & Strotz, L. (2011) Expanding the proxy toolkit to help identify past events — Lessons from the 2004 Indian Ocean Tsunami and the 2009 South Pacific Tsunami. *Earth-Science Reviews*, 107, 107–122. Available at: https://doi.org/10.1016/j.earscirev.2011.03.007

Dawson, A.G. (2000) Tsunami Deposits. *Pure and Applied Geophysics*, 157, 875–897. Available at: https://doi.org/10.1007/s000240050010

Dawson, A.G., Long, D. & Smith, D.E. (1988) The Storegga Slides: Evidence from eastern Scotland for a possible tsunami. *Marine Geology*, 82, 271–276. Available at: https://doi.org/10.1016/0025-3227(88)90146-6

Dawson, A.G., Smith, D.E. & Long, D. (1990) Evidence for a tsunami from a Mesolithic site in Inverness, Scotland. *Journal of Archaeological Science*, 17, 509–512. Available at: https://doi.org/10.1016/0305-4403(90)90031-y

Folk, R.L. & Ward, W.C. (1957) Brazos River bar [Texas]; a study in the significance of grain size parameters. *Journal of Sedimentary Research*, 27, 3–26. Available at: https://doi.org/10.1306/74D70646-2B21-11D7-8648000102C1865D

Hamilton, C.A., Lloyd, J.M., Barlow, N.L.M., Innes, J.B., Flecker, R. & Thomas, C.P. (2015) Late Glacial to Holocene relative sea-level change in Assynt, northwest Scotland, UK. *Quaternary Research*, 84, 214–222. Available at: https://doi.org/10.1016/j.yqres.2015.07.001

Harkness, D.D. (1983) The extent of natural 14C deficiency in the coastal environment of the United Kingdom. *PACT*, 8, 351–364.

Heaton, T.J., Köhler, P., Butzin, M., Bard, E., Reimer, R.W., Austin, W.E.N. et al. (2020) Marine20—The Marine Radiocarbon Age Calibration Curve (0–55,000 cal BP). *Radiocarbon*, 62, 779–820. Available at: https://doi.org/10.1017/RDC.2020.68

Hill, J. (2019) HRDS: A Python package for hierarchical raster datasets. *Journal of Open Source Software*, 4, 1112. Available at: https://doi.org/10.21105/joss.01112

Hill, J., Collins, G.S., Avdis, A., Kramer, S.C. & Piggott, M.D. (2014) How does multiscale modelling and inclusion of realistic palaeobathymetry affect numerical simulation of the Storegga Slide tsunami? *Ocean Modelling*, 83, 11–25. Available at: https://doi.org/10.1016/j.ocemod.2014.08.007

Intermap Technologies, 2007. NEXTMAP British Digital Terrain Model Dataset Produced by Intermap.

Jordan, J.T., Smith, D.E., Dawson, S. & Dawson, A.G. (2010) Holocene relative sea-level changes in Harris, Outer Hebrides, Scotland, UK. *Journal of Quaternary Science*, 25, 115–134. Available at: https://doi.org/10.1002/jqs.1281

Juggins, S. & Birks, H.J.B. (2012) Quantitative environmental reconstructions from biological data, In: *Tracking Environmental Change Using Lake Sediments*. Springer. pp. 431–494.

Kärnä, T., de Brye, B., Gourgue, O., Lambrechts, J., Comblen, R., Legat, V. et al. (2011) A fully implicit wetting–drying method for DG-FEM shallow water models, with an application to the Scheldt Estuary. *Computer Methods in Applied Mechanics and Engineering*, 200, 509–524. Available at: https://doi.org/10.1016/j.cma.2010.07.001

Kärnä, T., Kramer, S.C., Mitchell, L., Ham, D.A., Piggott, M.D. & Baptista, A.M. (2018) Thetis coastal ocean model: discontinuous Galerkin discretization for the three-dimensional hydrostatic equations. *Geoscientific Model Development*, 11, 4359–4382. Available at: https://doi.org/10.5194/gmd-11-4359-2018

Kemp, A.C. & Telford, R.J. (2015) Transfer functions, In: *Handbook of Sea-Level Research*. John Wiley & Sons, Ltd. pp. 470–499. https://doi.org/10.1002/9781118452547.ch31

Kucera, M., Weinelt, M., Kiefer, T., Pflaumann, U., Hayes, A., Weinelt, M. et al. (2005) Reconstruction of sea-surface temperatures from assemblages of planktonic foraminifera: multi-technique approach based on geographically constrained calibration data sets and its application to glacial Atlantic and Pacific Oceans. *Quaternary Science Reviews*, 24, 951–998. Available at: https://doi.org/10.1016/j.quascirev.2004.07.014

Lloyd, J. (2000) Combined foraminiferal and thecamoebian environmental reconstruction from an isolation basin in NW Scotland: Implications for sea-level studies. *The Journal of Foraminiferal Research*, 30, 294–305. Available at: https://doi.org/10.2113/0300294

Lloyd, J.M. & Evans, J.R. (2002) Contemporary and fossil foraminifera from isolation basins in northwest Scotland. *Journal of Quaternary Science*, 17, 431–443. Available at: https://doi.org/10.1002/jqs.719

Lo Giudice Cappelli, E. & Austin, W.E.N. (2020) Marine Bivalve Feeding Strategies and Radiocarbon Ages in Northeast Atlantic Coastal Waters. *Radiocarbon*, 62, 107–125. Available at: https://doi.org/10.1017/RDC.2019.68

Long, A.J., Barlow, N.L.M., Dawson, S., Hill, J., Innes, J.B., Kelham, C. et al. (2016) Lateglacial and Holocene relative sea-level changes and first evidence for the Storegga tsunami in Sutherland, Scotland. *Journal of Quaternary Science*, 31, 239–255. Available at: https://doi.org/10.1002/jqs.2862

Neill, S.P., Scourse, J.D. & Uehara, K. (2010) Evolution of bed shear stress distribution over the northwest European shelf seas during the last 12,000 years. *Ocean Dynamics*, 60, 1139–1156. Available at: https://doi.org/10.1007/s10236-010-0313-3

Reimer, P.J., Austin, W.E.N., Bard, E., Bayliss, A., Blackwell, P.G., Bronk Ramsey, C. et al. (2020) The IntCal20 Northern Hemisphere Radiocarbon Age Calibration Curve (0–55 cal kBP). *Radiocarbon*, 62, 725–757. Available at: https://doi.org/10.1017/RDC.2020.41

Reimer, P.J. & Reimer, R.W. (2001) A Marine Reservoir Correction Database and On-Line Interface. *Radiocarbon*, 43, 461–463. Available at: https://doi.org/10.1017/S0033822200038339

Selby, K.A. & Smith, D.E. (2007) Late Devensian and Holocene relative sea-level changes on the Isle of Skye, Scotland, UK. *Journal of Quaternary Science*, 22, 119–139. Available at: https://doi.org/10.1002/jqs.1012

Selby, K.A. & Smith, D.E. (2016) Holocene Relative Sea-Level Change on the Isle of Skye, Inner Hebrides, Scotland. *Scottish Geographical Journal*, 132, 42–65. Available at: https://doi.org/10.1080/14702541.2015.1051102

Selby, K.A., Smith, D.E., Dawson, A.G. & Mighall, T.M. (2000) Late Devensian and Holocene relative sea level and environmental changes from an isolation basin in southern Skye. *Scottish Journal of Geology*, 36, 73–86. Available at: https://doi.org/10.1144/sjg36010073

Shennan, I., Bradley, S.L. & Edwards, R. (2018) Relative sea-level changes and crustal movements in Britain and Ireland since the Last

Glacial Maximum. *Quaternary Science Reviews*, 188, 143–159. Available at: https://doi.org/10.1016/j.quascirev.2018.03.031

Shennan, I., Hamilton, S., Hillier, C. & Woodroffe, S. (2005) A 16,000-year record of near-field relative sea-level changes, northwest Scotland, United Kingdom. *Quaternary International*, 133-134, 95–106. Available at: https://doi.org/10.1016/j.quaint.2004.10.015

Shennan, I., Innes, J.B., Long, A.J. & Zong, Y. (1994) Late Devensian and Holocene relative sea-level changes at Loch nan Eala, near Arisaig, northwest Scotland. *Journal of Quaternary Science*, 9, 261–283. Available at: https://doi.org/10.1002/jqs.3390090307

Shennan, I., Innes, J.B., Long, A.J. & Zong, Y. (1995a) Late Devensian and Holocene relative sea-level changes in northwestern Scotland: New data to test existing models. *Quaternary International*, 26, 97–123. Available at: https://doi.org/10.1016/1040-6182(94)00050-F

Shennan, I., Innes, J.B., Long, A.J. & Zong, Y. (1995b) Holocene relative sea-level changes and coastal vegetation history at Kentra Moss, Argyll, northwest Scotland. *Marine Geology, Coastal Evolution in the Quarternary: IGCP Project*, 274(124), 43–59. Available at: https://doi.org/10.1016/0025-3227(95)00031-S

Shennan, I., Lambeck, K., Horton, B., Innes, J., Lloyd, J., McArthur, J. et al. (2000) Late Devensian and Holocene records of relative sea-level changes in northwest Scotland and their implications for glacio-hydro-isostatic modelling. *Quaternary Science Reviews*, 19, 1103–1135. Available at: https://doi.org/10.1016/S0277-3791(99)00089-X

Shennan, I., Rutherford, M.M., Innes, J.B. & Walker, K. (1996) Late glacial sea level and ocean margin environmental changes interpreted from biostratigraphic and lithostratigraphic studies of isolation basins in northwest Scotland. In: Andrews, J.T., Austin, W.E.N., Bergsten, H. & Jennings, A.E., (Eds.) *Late Quaternary of the North Atlantic Margins*, 111. London: Geological Society Special Publications. pp. 229–244.

Shennan, I., Tooley, M., Green, F., Innes, J., Kennington, K., Lloyd, J. et al. (1998) Sea level, climate change and coastal evolution in Morar, northwest Scotland. *Geologie en Mijnbouw*, 77, 247–262. Available at: https://doi.org/10.1023/A:1003690921945

Shennan, I. & Woodroffe, S.A. (2003) Holocene sea-level changes around Loch Duich and Loch Alsh, Northwest Highlands, In: *The Quaternary of Glen Affric and Kintail*. Quaternary Research Association. pp. 123–124.

Smith, D. (2004) The Holocene storegga slide tsunami in the United Kingdom. *Quaternary Science Reviews*, 23, 2291–2321. Available at: https://doi.org/10.1016/j.quascirev.2004.04.001

Smith, D.E., Barlow, N.L.M., Bradley, S.L., Firth, C.R., Hall, A.M., Jordan, J.T. et al. (2019) Quaternary sea level change in Scotland. *Earth and Environmental Science Transactions of The Royal Society of Edinburgh*, 110, 219–256. Available at: https://doi.org/10.1017/S1755691017000469

Smith, D.E., Cullingford, R.A. & Haggart, A. (1985) A Major Coastal Flood During the Holocene in Eastern Scotland. *E&G Quaternary Science Journal*, 35, 109–118. Available at: https://doi.org/10.3285/eg.35.1.14

Smith, D.E., Foster, I.D.L., Long, D. & Shi, S. (2007) Reconstructing the pattern and depth of flow onshore in a palaeotsunami from associated deposits. *Sedimentary Geology*, 200, 362–371. Available at: https://doi.org/10.1016/j.sedgeo.2007.01.014

Stuiver, M., Reimer, P.J., 1993. Extended14C Data Base and Revised CALIB 3.014C Age Calibration Program. *Radiocarbon* 35, 215–230. https://doi.org/10.1017/S0033822200013904